HHS Public Access

Author manuscript

Adv Funct Mater. Author manuscript; available in PMC 2019 April 17.

Published in final edited form as:

Adv Funct Mater. 2018 April 17; 28(16): . doi:10.1002/adfm.201707030.

Protoporphyrin IX (PpIX)-Coated Superparamagnetic Iron Oxide Nanoparticle (SPION) Nanoclusters for Magnetic Resonance Imaging and Photodynamic Therapy

Dr. Lesan Yan,
Department of Bioengineering, University of Pennsylvania, Philadelphia, PA 19104, USA

Dr. Ahmad Amirshaghaghi,
Department of Bioengineering, University of Pennsylvania, Philadelphia, PA 19104, USA

Dennis Huang,
Department of Bioengineering, University of Pennsylvania, Philadelphia, PA 19104, USA

Joann Miller,
Department of Radiation Oncology, Perelman School of Medicine, University of Pennsylvania, Philadelphia, PA 19104, USA

Prof. Joel M. Stein,
Department of Radiology, University of Pennsylvania, PA 19104, USA

Prof. Theresa M. Busch,
Department of Radiation Oncology, Perelman School of Medicine, University of Pennsylvania, Philadelphia, PA 19104, USA

Prof. Zhiliang Cheng, and
Department of Bioengineering, University of Pennsylvania, Philadelphia, PA 19104, USA

Andrew Tsourkas
Department of Bioengineering, University of Pennsylvania, Philadelphia, PA 19104, USA

Abstract

The ability to produce nanotherapeutics at large-scale with high drug loading efficiency, high drug loading capacity, high stability, and high potency is critical for clinical translation. However, many nanoparticle-based therapeutics under investigation suffer from complicated synthesis, poor reproducibility, low stability, and high cost. In this work, a simple method for preparing multifunctional nanoparticles is utilized that act as both a contrast agent for magnetic resonance imaging and a photosensitizer for photodynamic therapy for the treatment of cancer. In particular, the photosensitizer protoporphyrin IX (PpIX) is used to solubilize small nanoclusters of

Correspondence to: Zhiliang Cheng; Andrew Tsourkas.

The ORCID identification number(s) for the author(s) of this article can be found under https://doi.org/10.1002/adfm.201707030.

Conflict of Interest
The authors declare no conflict of interest.

Supporting Information
Supporting Information is available from the Wiley Online Library or from the author.

superparamagnetic iron oxide nanoparticles (SPIONs) without the use of any additional carrier materials. These nanoclusters are characterized with a high PpIX loading efficiency; a high loading capacity, stable behavior; high potency; and a synthetic approach that is amenable to large-scale production. In vivo studies of photodynamic therapy (PDT) efficacy show that the PpIX-coated SPION nanoclusters lead to a significant reduction in the growth rate of tumors in a syngeneic murine tumor model compared to both free PpIX and PpIX-loaded poly(ethylene glycol)-polycaprolactone micelles, even when injected at 1/8th the dose. These results suggest that the nanoclusters developed in this work can be a promising nanotherapeutic for clinical translation.

Keywords

magnetic resonance imaging; nanoclusters; photodynamic therapy; protoporphyrin; superparamagnetic iron oxide nanoparticles

1. Introduction

Recently, there has been growing interest in the development of multifunctional nanoparticles that combine therapeutic and diagnostic functions into a single nanoformulation.[1] To date, numerous methods have been used to prepare multifunctional nanoparticles. In most cases, drugs and imaging agents are coloaded into nanoparticles, and these particles have been based on a wide range of platforms including liposomes,[2] polymeric micelles/vesicles,[3] and organic/inorganic colloids.[4] These nanocarriers are typically water-soluble, biocompatible, biodegradable, and have a prolonged circulation time with enhanced tumor accumulation, allowing them to function as effective carriers for drugs and imaging agents. Despite the numerous benefits of these multifunctional nanoparticles, many nanoformulations that are under development suffer from complicated synthesis, poor reproducibility, and high cost. Moreover, most multifunctional nanoparticles require the use of carrier materials to solubilize the drugs and/or imaging agents. These carrier materials often make up the major weight fraction of the nanoparticle (typically > 80% of the weight), [5] thus limiting the drug loading capacity and increasing the number of nanoparticles that must be administered. This can increase the viscosity and osmolality of the injected nanoformulations and leads to adverse rheological effects.[6] The carrier material itself and/or its degradation products can also exhibit an undesirable toxic or immunogenic response.[7] Therefore, it is preferable to create nanotherapeutics that can be produced at large-scale, with high drug loading efficiency, high drug loading capacity (i.e., minimal carrier material), high stability, and high potency.

Photodynamic therapy (PDT) is a minimally invasive approach for cancer treatment that can be highly selective.[8] It uses photosensitizers to produce singlet oxygen upon the administration of light to kill cancer cells in the illuminated area.[9] Studies have shown that PDT is significantly less invasive than surgery, yet can be equally as effective.[10] In addition, PDT does not produce any of the long-term side effects that have been associated with radiation therapy.[11] As a result, PDT can provide tremendous advantages over conventional cancer treatment procedures.

Of the various photosensitizers, protoporphyrin IX (PpIX) is one of the most commonly used porphyrins in PDT.[12] PpIX is an organic compound formed from 5-aminole-vulimic acid (ALA) molecules. 5-ALA is the first compound in the pathway that leads to heme and chlorophyll, making PpIX a naturally occurring precursor of heme.[13] However, the intrinsically poor water solubility of PpIX makes the direct intravenous administration a challenge. Therefore, improving the PDT efficiency of this photosensitizer by optimizing the delivery protocol has been a widely pursued aim.

Many multifunctional nanoparticles have been developed for image-guided photodynamic/photothermal therapy, including functionalized graphene nanosheets anchored with magnetic nanoparticles,[14] intrabilayer ^{64}Cu labeling of photoactivatable, doxorubicin-loaded stealth liposomes,[15] photosensitizer-loaded gold vesicles,[16] and lanthanide-doped nanoparticles.[17] Superparamagnetic iron oxide nanoparticles (SPIONs) have attracted extensive interest for inclusion in multifunctional nanoparticles due to their superparamagnetic properties and ability to serve as magnetic resonance (MR) contrast agents.[18] SPIONs are able to generate strong T2 contrast and as such have been tested in a wide range of biomedical applications.[19] Due to the biocompatibility and biodegradability of SPIONs, numerous SPION nanoformulations have already been evaluated in humans, with some already approved for clinical use.[20]

Combining both diagnostic SPIONs for MR imaging and PpIX for PDT within a single nanoformulation could provide a novel therapeutic strategy for cancer treatment. In particular, high resolution MR imaging can be used to visualize the localization and accumulation of the nanoparticle within the tumor, which can guide the administration of PDT. Various nanocarriers have previously been adopted to codeliver SPIO and photosensitizers, e.g, phospholipid liposomes and polymeric nanoparticles;[21] however, many of the above-mentioned challenges hinder their clinical translation. Therefore, the development of a codelivery system with high drug loading capacity (i.e., minimum use of carrier materials), high stability, and effective MR contrast is highly desired. Based on these considerations, we developed carrier-free PpIX-coated SPION nanoclusters. These nanoclusters were systemically characterized in vitro and in vivo in terms of their contrast enhancing capabilities and their therapeutic efficacy.

2. Results and Discussion

2.1. Synthesis and Characterization of PpIX-Coated SPION Nanoclusters

PpIX-coated SPION nanoclusters (Figure 1) were formed by simply dissolving PpIX and small hydrophobic SPIONs (diameter = 7.3 ± 1.0 nm; Figure S1, Supporting Information) in an organic solvent, adding this mixture to water, and sonicating to create an oil-in-water microemulsion. The organic solvent was removed under vacuum, followed by dialysis. The nanoclusters were further purified from free PpIX by magnetic column purification. The resulting nanoclusters were highly soluble in aqueous solutions, with the amphiphilic PpIX molecules bound to the surface via hydrophobic interactions and acting as a stable coating material without the use of any additional amphiphilies or carrier materials. As a comparison, use of SPIONs-alone, i.e., without PpIX, led to a rapid nanoparticle

precipitation in aqueous solutions (Figure S2, Supporting Information), confirming that PpIX was needed for the solubilization of nanoclusters in water.

The PpIX-coated SPION nanoclusters had an average hydrodynamic diameter of ≈37 nm with a polydispersity index (PDI) of 0.22 in water based on dynamic light scattering measurements (Figure 2A). Transmission electron microscopy (TEM) images showed that the SPIONs were tightly packed into a spherical core (Figure 2A inset), with overall diameters that were in good agreement with dynamic light scattering (DLS) measurements. The nanoclusers exhibited superparamagnetic properties with an r2 value of 222 ± 11 mM^{-1} s^{-1} (Figure 2B). In vitro MR imaging of nanoclusters showed enhanced T2-contrast (i.e., hypointensity) compared to the control samples (Figure 2B inset). The nanocluster yield was >90%, based on the recovery of SPION, and the loading efficiency of PpIX was >80%, when the PpIX:Fe ratio (w/w) was at 1:2. A further increase in the ratio of PpIX:Fe during synthesis did not result in a significant increase in PpIX per cluster, but rather reduced the PpIX loading efficiency. All subsequent studies were performed at a PpIX:Fe ratio of 1:2.

2.2. PpIX-Coated SPION Nanocluster Reproducibility

The oil-in-water microemulsion method that was used to produce the PpIX nanoclusters was highly reproducible three independent batches of nanoclusters were prepared, the average hydrodynamic diameter was 36.89 nm with a standard deviation of just 2.71 nm. The average PDI was 0.223 with a standard deviation of 0.006. The average relaxivity of the three independent batches was 222 mM^{-1} s^{-1} with a standard deviation of 11 mM^{-1} s^{-1} (Figure 3B, Table S1 in the Supporting Information). Similar PpIX loading efficiencies (85–90%) were also found in the three independent nanocluster batches, based on UV-spectroscopy.

2.3. Stability of PpIX-Coated SPION Nanoclusters

The stability of the PpIX-coated nanoclusters was evaluated in water and fetal bovine serum. There was no observable change in the hydrodynamic diameter or in the T2 relaxation time of the nanocluster samples in water for at least one week (Figure 4A) indicating that there is no aggregation or precipitation of the nanoclusters over this time period. Further, there was no change in the UV-absorption spectrum or any detectable dissociation of the PpIX from the nanoclusters in water, over one week (Figure 4B).

When the nanoclusters were incubated in serum for 72 h at 37 °C, there was an initial increase in the hydrodynamic diameter of the nanocluster from ≈37 to ≈60 nm, most likely due to opsonization and formation of a protein corona, but there was no significant change in the hydrodynamic diameter thereafter. There was also no change in the T2 relaxation time (Figure 4C). Some PpIX did dissociate from the nanoclusters over the course of the three day experiment (Figure 4D), but ≈75% of the PpIX remained associated with the SPIONs and thus the nanoclusters were deemed sufficiently stable for in vivo use, compared with ≈50% release from PpIX loaded poly(ethylene glycol)-polycaprolactone (PEG-PCL) micelles in serum.[12] Dissociation of PpIX from the nanoclusters could lead to some discrepancy between the MR signal and PpIX localization in living subjects; however, the

MR signal is still expected to be a good qualitative indicator of PpIX accumulation within tumors, due to the high nanocluster stability.

2.4. PDT Efficacy of PpIX-Coated SPION Nanocluster in 4T1 Cancer Cells

The cytotoxicity of the PpIX-coated SPION nanoclusters on 4T1 breast cancer cells was studied via 3-(4,5-dimethylthiazol-2-yl)-2,5-diphenyltetrazolium bromide (MTT) assay under dark conditions (no illumination; dark controls) and in the presence of illumination (i.e., PDT). Cell viability was measured as the percentage of the viable cells compared with untreated control cells (i.e., without nanoclusters and without PDT). As seen in Figure S3 (Supporting Information), PpIX-coated SPION nanoclusters showed an increase in fluorescence intensity from 0.5 to 24 h, indicating the nanoparticle cellular uptake. No cytotoxicity was observed with PpIX-coated SPION nanoclusters in the absence of PDT for all doses of nanoparticle that were tested (up to a PpIX concentration of 20 μg mL^{-1}). In contrast, with PDT, the cell viability decreased with increasing concentrations of the nanocluster before plateauing at ≈20% cell viability at a PpIX concentration of 5 μg mL^{-1} (Figure 5). Thus, PpIX-coated SPION nanoclusters did not lead to dark toxicity at doses of ≤20 μg mL^{-1} (maximum tested dose), but were highly effective in presence of illumination to produce PDT-mediated cellular damage. Similar phenomenon has also been observed for the free PpIX (Figure S4 in the Supporting Information).

2.5. Magnetic Resonance Imaging

Since most solid tumors exhibit hypervascularity, leaky vascular architecture, and the absence of effective lymphatic drainage, macromolecules and nanometer-sized particles can accumulate preferentially at tumor sites through a passive targeting effect, known as the enhanced permeability and retention effect.[22] To monitor the accumulation of PpIX-coated SPION nanoclusters in a syngeneic orthotopic tumor model, the mouse breast cancer cell line 4T1 was implanted in the right mammary fat pad in BALBC/cAnNCr mice. T2-weighted MR images were acquired immediately prior to injection of nanoclusters and 24 h after injection at a dose of 5 mg Fe per kg body weight. The post-contrast image revealed a notable loss in signal (i.e., hypointensity) in the tumor (Figure 6A), indicative of nanocluster accumulation within the tumor. The MR signal in the tumor regions of interest was also analyzed quantitatively (Figure 6B). Signal-to-background ratio (SBR) measurements were made using the tumor and the water as background. The postinjection SBR was significantly lower at 0.33 +/− 0.08 compared to preinjection SBR of 1.10 +/− 0.16, $p < 0.001$ (Figure 6B).

2.6. PDT Animal Studies

The efficacy of the PpIX-coated SPION nanoclusters as a PDT agent was also evaluated using a 4T1 syngeneic orthotopic tumor model. For tumor propagation, 4T1 cells were implanted in the right mammary fat pad in BALBC/cAnNCr mice. Seven days postinoculation, when the tumors had reached ≈50 mm^3 in size, the mice were divided into 7 groups ($n = 5$): (1) untreated control; (2) PpIX; (3) PpIX + light (PDT); (4) PpIX-loaded PEG-PCL micelles; (5) PpIX-loaded PEG-PCL micelle + light (PDT); (6) PpIX-coated SPION nanoclusters; (7) PpIX-coated SPION nanoclusters + light (PDT). The mice were given an intravenous injection of PpIX or PpIX-loaded PEG-PCL micelle at a dose of 40 mg

per kg PpIX or PpIX-coated SPION nanoclusters at a dose of 5 mg per kg PpIX. The photosensitizer was delivered on day 0 and light was delivered on day 1 to all groups. Tumor size was subsequently measured on a daily basis. Interestingly, none of the treatments had an effect on the rate of tumor growth, except when PDT was combined with the PpIX-coated SPION nanoclusters. The tumor growth in this group was significantly slower than tumor-bearing animals that received PDT in combination with free PpIX and PpIX-loaded PEG-PCL micelles (Figure 7), despite receiving an eightfold lower dose of PpIX. The PpIX-coated SPION nanoclusters showed no obvious influence on mouse body weight (Figure S5 in the Supporting Information).

2.7. Discussion

A successful nanocluster synthesis protocol has been established utilizing PpIX and SPIONs. The generated nanoclusters are stable and robust in both storage and physiological conditions. The amphiphilic properties of PpIX allow for the hydrophobic domains to be orientated around the SPIO cores, while the hydrophilic domains are in contact with the physiological environment. The procedure for the synthesis of PpIX-coated SPION nanoclusters is highly reproducible based on relaxometry measurements, DLS size measurements, and UV-absorption spectroscopy. The TEM images indicate densely packed SPIONs that form a spherical nanocluster with an overall diameter of ≈37 nm. DLS measurements suggest that the polydispersity of the nanoclusters is low. The nanoclusters are stable in both water and physiological samples (e.g., serum). In vitro release studies indicate that the vast majority of the PpIX stays associated with the nanocluster, even in serum. MTT studies revealed that the PpIX-coated SPION nanoclusters were non-toxic without light and would significantly reduce cell viability once exposed to light.

Promising results during characterization, stability and release studies, and cell studies prompted PDT studies in a syngeneic orthotopic murine breast tumor model. A significant reduction in the rate of tumor growth was observed when PpIX-coated SPION nanoclusters were used for PDT, compared to untreated controls, despite being at 1/8th the dose. The tumor volume was reduced by 82.60% compared to PDT with free PpIX at 9 d posttreatment. Similarly, PDT with the PpIX-coated SPION clusters led to a reduction in tumor volume by 87.12% compared to treatment with PpIX-loaded PEG-PCL micelles. It is speculated that the improved efficacy of the PpIX-coated nanoclusters stems from their enhanced stability. Amphiphilic species like PpIX are prone to leak out of micelles and thus it is likely that very little of the drug is delivered to the tumor site. These initial animal study results indicate promising improvements to PDT applications, as well as improved efficiency for targeted drug delivery.

3. Conclusion

In conclusion, we developed a novel nanotherapeutic platform for magnetic resonance imaging and photodynamic therapy. Our nanoplatform is quite unique because it is formulated with only PpIX and SPIONs. No additional stabilizing materials were introduced. The PpIX-coated SPION nanoclusters are stable in vitro and in physiological conditions. The characteristics of these clusters are highly reproducible and utilize two low-

cost components in a simple protocol. The nanoclusters show encouraging imaging and therapeutic potential and may be a promising agent for clinical translation.

4. Experimental Section

Materials

Poly(ethylene glycol) (4000)- polycaprolactone (3000) copolymer (denoted PEG-PCL) was purchased from Polymer Source (Dorval, Quebec, Canada). PpIX was purchased from Sigma-Aldrich (St. Louis, MO). Cell culture medium (Dulbecco's Modified Eagle Medium), penicillin, streptomycin, and heat-inactivated fetal bovine serum (FBS) were purchased from Gibco Life Technologies, Inc. (Grand Island, NY, USA). All of the buffer solutions were prepared with deionized water. PpIX-loaded PEG-PCL micelles were prepared as previously described.[12] All other chemicals were used as received.

Preparation of Superparamagnetic Iron Oxide Nanoparticles

SPION were prepared by thermal decomposition as previously described.[23] Briefly, a mixture of iron(III) acetylacetonate [$Fe(acac)_3$] (2 mmol), 1,2-hexadecanediol (5 mmol), oleic acid (2 mmol), oleylamine (6 mmol), and benzyl ether (20 mL) was heated and stirred under nitrogen at 200 °C for 15 min. Then, the mixture under nitrogen was heated to reflux (300 °C) for 1 h and allowed to cool back to room temperature. Nanoparticles were precipitated by adding two volumes of ethanol to the mixture and centrifuged at 5500 × g for 15 min. The nanoparticles were allowed to air dry before dissolving in toluene. Large aggregates were removed via centrifugation at 3000 × g for 15 min.

Preparation of PpIX-Coated SPION Nanoclusters

1 mg PpIX was mixed with 50 μL dimethyl sulfoxide (DMSO), with the addition of SPIO (2.2 mg based on the Fe concentration in toluene) in 150 μL toluene, and then vortexed at 50 °C until PpIX and SPIO were fully dissolved. Next, this mixture was injected into a glass vial containing 4 mL of water. The sample was sonicated until the solution became homogenous. The glass vial was placed in a dark environment and left open to allow the toluene to evaporate overnight. Dialysis was performed in 4 L of water overnight to remove DMSO and any unloaded PpIX from the sample. The formed PpIX-coated SPION clusters were centrifuged at 1000 × g for 15 min, and then purified by PD-10 column. The synthesized clusters were characterized by UV-absorption spectroscopy (Varian, 100 Bio), dynamic light scattering (Malvern, Zetasizer, Nano-ZS), transmission electron microscopy (JOEL 1010), and relaxometry (Bruker, mq60 NMR analyzer). The PpIX encapsulation efficiency was calculated according to the following equation

$$\text{Encapsulation efficiency}\,(\%) = \frac{\text{Weight of PpIX in purified nanoparticles}}{\text{Weight of PpIX used in feed}} \times 100 \quad (1)$$

PpIX and iron concentration were quantified by UV-absorption and inductively coupled plasma optical emission spectrometry (ICP-OES), respectively.

PpIX-Coated SPION Nanoclusters Stability and Release Studies

Synthesized PpIX SPIO clusters were incubated in water as well as in FBS at 37 °C for the stability study. DLS was used to monitor the particle size over a total of one week. In addition, the amount of PpIX in the clusters was calculated over the same period of time by UV-absorption spectroscopy. Finally, aliquots taken from the sample were tested at various time points for the determination magnetic properties via T2.

In vitro release behavior of PpIX from clusters was investigated in FBS. Briefly, 0.5 mL as prepared PpIX-coated SPION nanoclusters in water were added to 9.5 mL FBS. The release experiment was initiated by placing the mixture at 37 °C with continuous shaking. At predetermined intervals, 0.5 mL solution was taken over 3 d and run through MACS normal columns ((25 LD columns, Miltenyi Biotec, Germany)) to separate free PpIX released from PpIX-coated SPION nanoclusters. UV-absorption spectroscopy was used to determine the amount of PpIX in the purified PpIX coated SPIO cluster samples. Normalized peak absorbance was measured over 3 d and the cumulative release percentage of PpIX was plotted as a function of incubation time.

MRI Phantom Imaging

Upon determining iron concentration of SPIO by ICP-OES, relaxometry measurements were performed in T2 mode (Varian, 4.7 Tesla) on a series of dilutions of the clusters. A plastic 120-well plate (MR phantom) was used to test the T2 hypointensity, indicating that abnormalities appear darker during MR imaging, associated with the synthesized PpIX-coated SPION nanocluster on a 4.7 T magnet.

Cell Culture

The mouse breast cancer cell line 4T1 (ATCC) was cultured and maintained in Dulbecco's Modified Eagle Medium (DMEM) containing 10% FBS, supplemented with 100 U mL^{-1} penicillin and 100 U mL^{-1} streptomycin at 37 °C with 5% CO_2.

Cellular Uptake Measured by Fluorescence Microscopy

Fluorescence microscopy was used to determine the cellular uptake behavior of PpIX coated SPION clusters. 4T1 cells were utilized upon seeding in a 6-well plate at a density of 5×10^5 cells per well. The cells were submerged in 2 mL of DMEM cell culture medium and incubated in a 5% CO_2 environment at 37 °C for 24 h. After incubation, the original culture medium was removed and incubated with PpIX coated SPION nanoclusters at a PpIX concentration of 5 μg mL^{-1} in newly added DMEM for 24 h. The cells were washed with cold phosphate buffer saline (PBS) to remove excess PpIX coated SPION nanoclusters that were not uptaken by the 4T1 cells. Microscopy images were taken with an Olympus IX81 motorized inverted fluorescence microscope with a back-illuminated EMCCD camera (Andor), an X-cite 120 excitation source, and Sutter excitation and emission filter wheels.

MTT Assay

In vitro cytotoxicity properties of free PpIX and PpIX-coated SPION nanoclusters were characterized by MTT assay against 4T1 cells. Cells harvested during their logarithmic

growth phase were seeded in 96-well plates (Greiner Bio-One, Alphen a/d Rijn, The Netherlands) at ≈5 × 10^3 cells per well. The 4T1 cells were incubated in 100 μL of DMEM cell culture medium at 37 °C in a 5% CO_2 environment for 24 h. The diluted free PpIX and PpIX-coated SPION nanoclusters were added to the wells at five different concentrations ranging from 20 to 1.25 μg mL^{-1} (20, 10, 5, 2.5, and 1.25 μg mL^{-1}). After 24 h incubation, the cells were illuminated with light delivered through microlens-tipped fibers (Pioneer, Bloomfield, CT) from a Ceralas diode laser (Biolitec AG, Jena, Germany; $\lambda = 632 \pm 3$ nm). Illumination was to a dose of 5 J cm^{-2} at power density of 5 mW cm^{-2} (1000 s), measured by a LabMaster Power Meter (Coherent, Auburn CA).

After irradiation, the 4T1 cells grew for an additional 24 h in DMEM before adding 10 μL of 5 mg per mL MTT assay stock solution to each well and incubating for 4 h. The formazan was dissolved by adding 100 μL of detergent to each well and then incubated for another 4 h. Finally, the plates were shaken for 1 min and the absorbance of formazan product was measured on a Tecan plate reader (Tecan) at 570 nm. Cell viability was calculated using the following equation

$$\text{Cell viability}\,(\%) = \frac{\text{Absorbance}_{\text{sample}}}{\text{Absorbance}_{\text{control}}} \times 100 \quad (2)$$

An internal negative control was prepared by keeping a portion of the wells covered during illumination to assess dark cytotoxicity.

Animal Studies

Animal investigations were approved by the Institutional Animal Care and Use Committee of the University of Pennsylvania. Studies of ≈6 week old female BALBC/cAnNCr mice (Charles River Laboratory, Charles River, MS, USA) were initiated by tumor propagation. Mice were anesthetized by isoflurane, and then injected subcutaneously with 4T1 cells in the right mammary fat pad (2 × 10^6 cells in 0.1 mL of PBS).

Control Balb/c mice with tumor volumes of ≈50 mm^3 were imaged by magnetic resonance imaging (MRI) at times pre and 24 h postinjection of PpIX-coated SPION nanoclusters (5 mg kg^{-1} via tail vein injection). Imaging parameters for preinjection and postinjection (gems, TR 200, TE 5, Flip 20) were matched and confirmed by an attending radiologist. Imaging analyses were performed on preinjection and postinjection images to compare the mean PpIX-coated SPION clusters at the tumor site.

For tumor response studies, 4T1 tumor volume was monitored daily and mice with a tumor volume of 50 mm^3 were randomly assigned to one of 7 groups (5 mice per group). These groups consisted of untreated animals, as well as animals that received free PpIX, PpIX-loaded PEG-PCL micelles, or PpIX-coated SPION nanoclusters as dark controls (no illumination) or in combination with illumination (i.e., PDT). Free PpIX and PpIX-loaded PEG-PCL micelles were delivered at a dose of 40 mg PpIX per kg body weight via tail vein injection at 24 h before light delivery. The PpIX-coated SPION nanoclusters were delivered

at a dose of 5 mg PpIX kg^{-1}. In anesthetized (isoflurane) animals, tumor growth on the mammary fat pad was surgically exposed by a single incision parallel to the palpable tumor and the tumor was illuminated by light delivery to a 1 cm diameter region that was centered on the tumor. This approach mimics standard clinical practice; however, in patients we could expect that surgery would precede PDT and light delivery would be to residual (undetected) disease. Immediately after PDT, the incision was closed with sutures. Light was produced by a diode laser (632 ± 3 nm; B&W Tek, Inc.) and delivered through microlens-tipped fibers (Pioneer). The intensity of the laser output was monitored and adjusted (LabMaster power meter; Coherent) to produce a fluence rate of 75 mW cm^{-2} at the tumor surface. Illumination was to a total fluence of 135 J cm^{-2} (30 min).

The tumor volume was monitored every other day by measuring the tumor length (major axis of the tumor) and width (minor axis of the tumor) with a caliper. The weight of the mice was also monitored over the period of posttreatment. The tumor volume was calculated using the following equation

$$\text{Tumor Volume}\,(V) = \text{length} \times (\text{width})^2/2 \quad (3)$$

The average tumor volume was determined within each experimental group and plotted against set time points to visualize the tumor growth curve.

Supplementary Material

Refer to Web version on PubMed Central for supplementary material.

Acknowledgments

This work was supported in part by the National Institutes of HealthR01NS100892 (Z.C.), R01CA175480 (Z.C.), R01CA181429 (A.T.), P01CA087971 (T.M.B.; project 4), P30CA016520 (Z.C.; T.M.B.; and A.T.) and R01CA085831 (T.M.B).

References

1. Cheng ZL, Al Zaki A, Hui JZ, Muzykantov VR, Tsourkas A. Science. 2012; 338:903. [PubMed: 23161990]
2. a) Park JH, Cho HJ, Yoon HY, Yoon IS, Ko SH, Shim JS, Cho JH, Park JH, Kim K, Kwon IC, Kim DD. J Controlled Release. 2014; 174:98.b) Pacheco-Torres J, Mukherjee N, Walko M, Lopez-Larrubia P, Ballesteros P, Cerdan S, Kocer A. Nanomed-Nanotechnol. 2015; 11:1345.
3. a) Ding MM, Wei J, Wang R, Shuai XY, Li JH, Tan H, Fu Q. J Controlled Release. 2017; 259:E96.b) Muthiah M, Lee SJ, Moon M, Lee HJ, Bae WK, Chung IJ, Jeong YY, Park IK. J Nanosci Nanotechnol. 2013; 13:1626. [PubMed: 23755567]
4. a) Wang Z, Shao D, Chang Z, Lu M, Wang Y, Yue J, Yang D, Li M, Xu Q, Dong WF. ACS Nano. 2017; 11:12732. [PubMed: 29140684] b) Sun X, Du R, Zhang L, Zhang G, Zheng X, Qian J, Tian X, Zhou J, He J, Wang Y, Wu Y, Zhong K, Cai D, Zou D, Wu Z. ACS Nano. 2017; 11:7049. [PubMed: 28665575]
5. Tong R, Cheng JJ. Angew Chem, Int Ed. 2008; 47:4830.
6. Silva AC, Santos D, Ferreira DC, Souto EB. Pharmazie. 2009; 64:177. [PubMed: 19348340]

7. a) Nel A, Xia T, Madler L, Li N. Science. 2006; 311:622. [PubMed: 16456071] b) Dobrovolskaia MA, Mcneil SE. Nat Nanotechnol. 2007; 2:469. [PubMed: 18654343]
8. Chatterjee DK, Fong LS, Zhang Y. Adv Drug Delivery Rev. 2008; 60:1627.
9. Ortel B, Shea CR, Calzavara-Pinton P. Front Biosci. 2009; 14:4157.
10. Huang Z. Technol Cancer Res Treat. 2005; 4:283. [PubMed: 15896084]
11. DEJG, Dolmans J, Fukumura D, Jain RK. Nat Rev Cancer. 2003; 3:380. [PubMed: 12724736]
12. Yan L, Miller J, Yuan M, Liu JF, Busch TM, Tsourkas A, Cheng ZL. Biomacromolecules. 2017; 18:1836. [PubMed: 28437090]
13. Wachowska M, Muchowicz A, Firczuk M, Gabrysiak M, Winiarska M, Wanczyk M, Bojarczuk K, Golab J. Molecules. 2011; 16:4140.
14. Yang K, Hu LL, Ma XX, Ye SQ, Cheng L, Shi XZ, Li CH, Li YG, Liu Z. Adv Mater. 2012; 24:1868. [PubMed: 22378564]
15. Luo D, Goel S, Liu HJ, Carter KA, Jiang D, Geng J, Kutyreff CJ, Engle JW, Huang WC, Shao S, Fang C, Cai W, Lovell JF. ACS Nano. 2017; 11:12482. [PubMed: 29195037]
16. Lin J, Wang SJ, Huang P, Wang Z, Chen SH, Niu G, Li WW, He J, Cui DX, Lu GM, Chen XY, Nie ZH. ACS Nano. 2013; 7:5320. [PubMed: 23721576]
17. Park Y, Kim HM, Kim JH, Moon KC, Yoo B, Lee KT, Lee N, Choi Y, Park W, Ling D, Na K, Moon WK, Choi SH, Park HS, Yoon SY, Suh YD, Lee SH, Hyeon T. Adv Mater. 2012; 24:5755. [PubMed: 22915170]
18. Thorek DLJ, Chen A, Czupryna J, Tsourkas A. Ann Biomed Eng. 2006; 34:23. [PubMed: 16496086]
19. a) Laurent S, Forge D, Port M, Roch A, Robic C, Elst LV, Muller RN. Chem Rev. 2008; 108:2064. [PubMed: 18543879] b) Yoo D, Lee JH, Shin TH, Cheon J. Acc Chem Res. 2011; 44:863. [PubMed: 21823593]
20. Lin MM, Kim DK, El Haj AJ, Dobson J. IEEE Trans Nanobiosci. 2008; 7:298.
21. Luk BT, Fang RH, Zhang L. Theranostics. 2012; 2:1117. [PubMed: 23382770]
22. Maeda H, Wu J, Sawa T, Matsumura Y, Hori K. J Controlled Release. 2000; 65:271.
23. McQuade C, Al Zaki A, Desai Y, Vido M, Sakhuja T, Cheng ZL, Hickey RJ, Joh D, Park SJ, Kao G, Dorsey JF, Tsourkas A. Small. 2015; 11:834. [PubMed: 25264301]

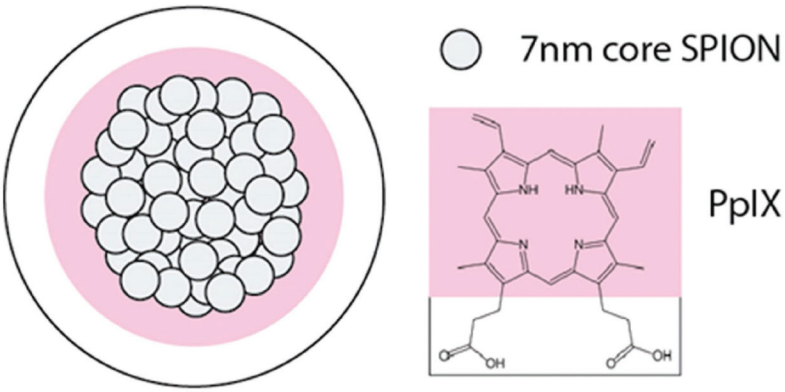

Figure 1.

Schematic diagram of PpIX-coated SPION nanoclusters. Clusters were formed through the coassembly of the small hydrophobic iron oxide nanoparticles (7 nm in diameter) and the photosensitizer photoporphyrin IX (PpIX). Due to amphiphilic property of PpIX, PpIX was coated onto the SPIO core that was able to solubilize SPIO nanoclusters.

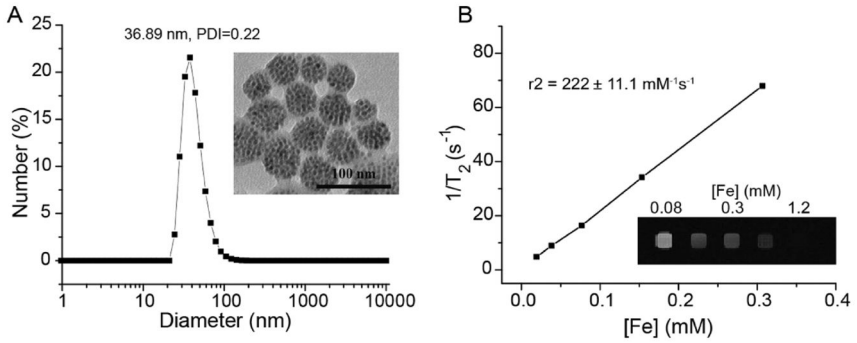

Figure 2.

A) Dynamic light scattering and transmission electron microscopy image (insert) of PpIX-coated SPION nanoclusters. B) Magnetic resonance (MR) relaxometry measurements of nanoclusters. MR phantom image (inset) of nanoclusters at various concentrations in a microplate was also collected.

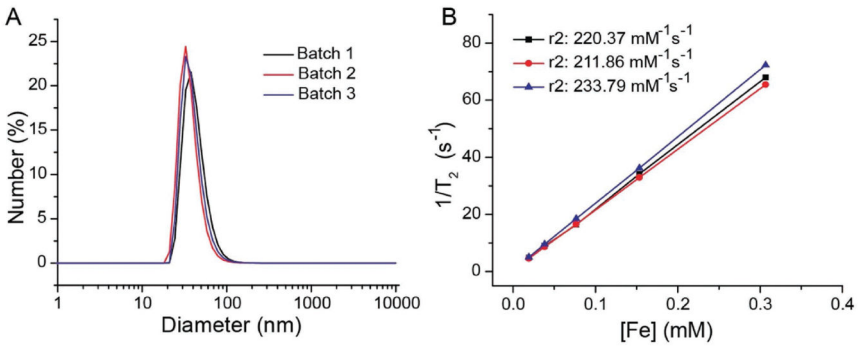

Figure 3.

Reproducibility of PpIX-coated SPION nanoclusters produced in the three separate batches. A) PpIX-coated SPION nanoclusters exhibited similar sizes shown by DLS measurements. B) Relaxation rate was reproducible across three batches of clusters with similar fit slopes.

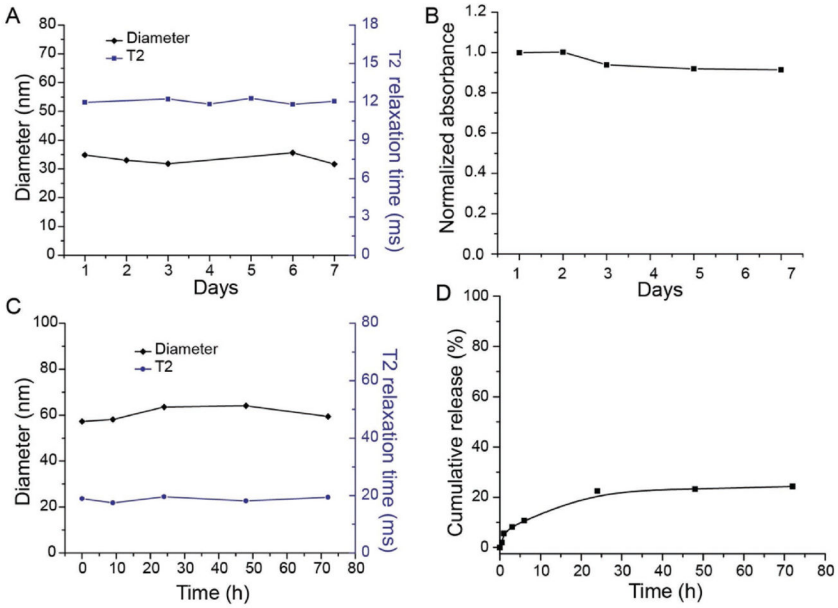

Figure 4.

Stability of PpIX-coated SPION nanoclusters. A) Nanoclusters were incubated in water, at 25 °C, and diameter and relaxometry measurements were recorded as a function of time. B) UV-absorption results of PpIX-coated SPION nanoclusters over time in water, 25 °C. C) Nanoclusters were incubated in serum, at 37 °C, and dynamic light scattering (DLS) and relaxometry measurements were recorded as a function of time. D) Release of PpIX from nanoclusters was monitored as a function of time following addition to serum, at 37 °C.

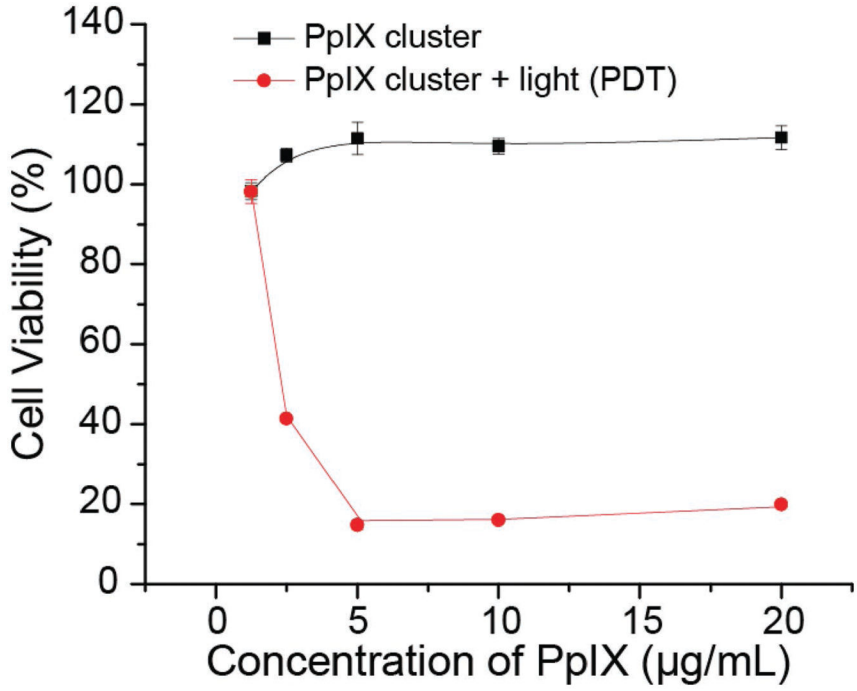

Figure 5.

Cell viability of 4T1 cells after treatment with PpIX-coated SPION nanoclusters at various PpIX concentrations in the absence (dark control) and presence of 632 nm illumination (PDT). Illumination was to a total dose of 5 J cm^{-2}. Data are presented as the average ± standard deviation ($n = 4$).

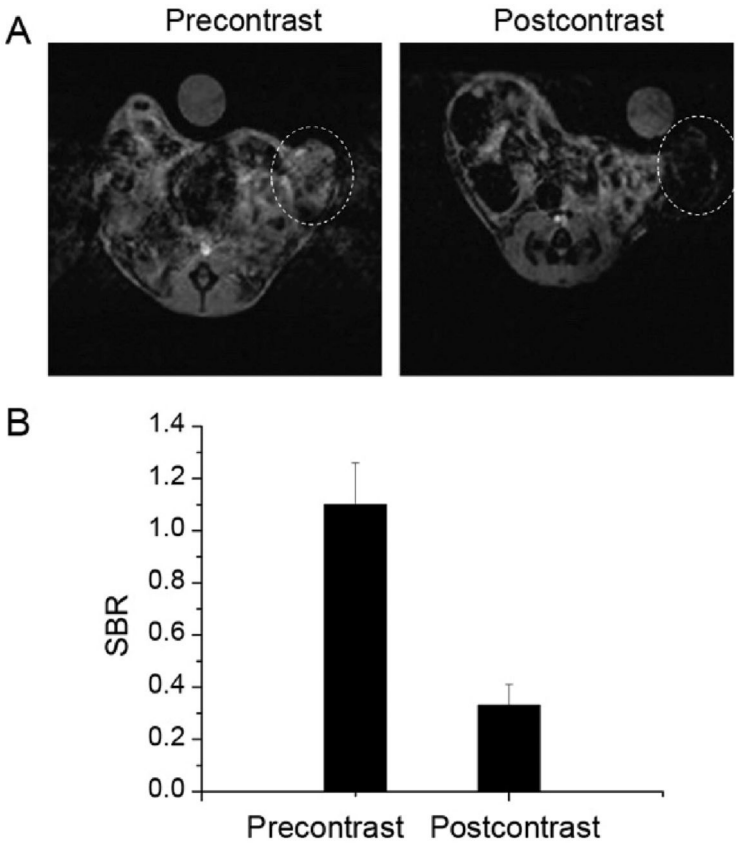

Figure 6.

In vivo MR images and signal intensity analysis of mice with 4T1 orthotopic tumor. A) T2-weighted magnetic resonance images in the axial plane prior to injection (precontrast) and 24 h after intravenous injection (postcontrast) of PpIX-coated SPION nanoclusters. Tumor location is indicated by dotted white circle. B) Quantitative analysis of MR images. Signal-to-background ratio (SBR) measurements were made using the tumor and the water as background. Preinjection versus postinjection SBR measurements are shown ($n = 3$ mice; columns represent SBR with error bars as standard deviation).

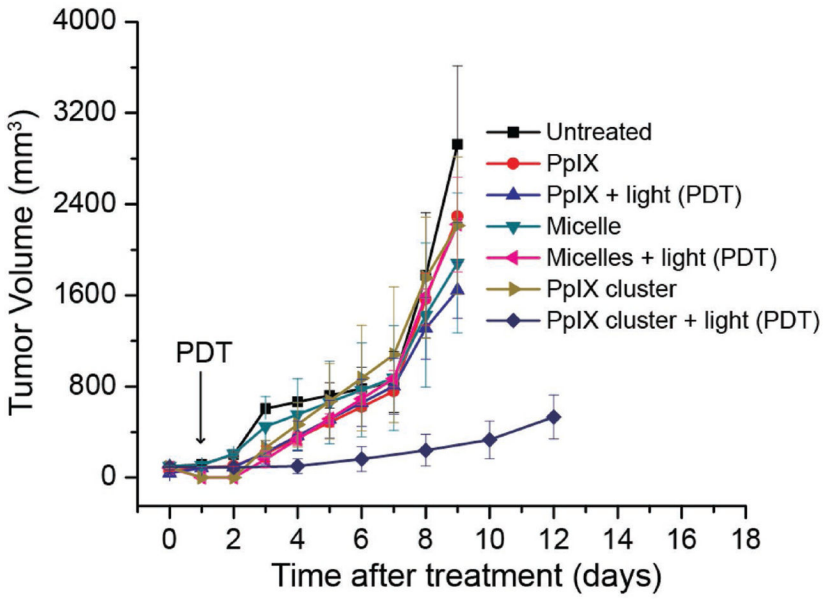

Figure 7.

In vivo antitumor activity after i.v. injection of PBS (untreated), free PpIX, PpIX-loaded PEG-PCL micelles at a PpIX concentration of 40 mg per kg body weight; PpIX-coated SPION nanoclusters at a PpIX concentration of 5 mg per kg body weight ($n = 5$). PDT of 4T1 tumors showed in vivo antitumor activity with delayed tumor growth when PpIX-coated SPION nanoclusters were used as the photodynamic agent after a single injection. Illumination (632 nm) was to a total fluence of 135 J cm^{-2} at a fluence rate of 75 mW cm^{-2}. Points indicate the average tumor volume of five mice with errors bar representing the standard deviation.